CrossMark

Study on metal decorated oxidized multiwalled carbon nanotube (MWCNT) - epoxy adhesive for thermal conductivity applications

Amit K. Singh[1,2] · Bishnu P. Panda[1] · Smita Mohanty[1,2] · Sanjay K. Nayak[1,2] ·
Manoj K. Gupta[3]

Abstract In this work, an effort has been made to develop a new type of complex conductive adhesive filled with silver decorated multi-walled carbon nanotubes (Ag-MWCNT). MWCNTs have been modified using *N,N*-dimethyl formamide (DMF) as a reducing agent and silver nanoparticles (Ag-NPs) has been homogeneously decorated against the surface. Fourier transform infra-red spectroscopy (FTIR) and Raman spectroscopy concluded that carboxylic groups were anchored to the surface of nanotubes. X-ray diffraction (XRD), transmission electron microscopy (TEM) and energy-dispersive spectroscopy (EDS) confirmed that Ag-NPs were formed and uniformly deposited onto the surface of carboxylic functionalized MWCNT. Test results indicated an improvement in the thermal conductivity up to 0.88 W/mK, which was about four-fold increase over pristine epoxy. The curing kinetics of Ag-MWCNTs reinforced epoxy adhesive system was also studied using non-isothermal differential scanning calorimetric (DSC) technique. The activation energy obtained by Kissinger's method was reduced from 57.2 to 54 kJ/mol with an addition of 0.5 wt% of Ag-MWCNT within unmodified epoxy. Lap shear strength of the adhesive containing 0.5 wt% of Ag-MWCNT was higher than the pristine polymer thus confirming reinforcing effect of Ag-MWCNT in conductivity applications.

1 Introduction

Thermally conductive adhesives (TCAs) are significant weapon in the war against heat raging within today's powerful electronic devices. TCAs with advanced performance characteristics are extensively used as an alternative to lead/tin solders in electrical and electronics binding applications. In particular, with the desire for making of superior interconnects in advanced packaging, nano-conductive adhesives are becoming more vital due to the special electrical, chemical, mechanical, magnetic and optical properties that nano-sized materials can possess. Therefore, there has been an extensive research for the last few years on the advances of nano-conductive adhesives that contain nano-filler such as nanoparticles, CNTs and monolayer graphenes [1, 2].

Epoxy based conductive adhesives are common interface materials for electronic packaging due to their well-known ability to accept wide range of fillers. Epoxy based conductive adhesives are utilized in the fabrication of LEDs attachment and computer machinery. A further application consists of printed circuit board fabrication [3], advanced material composites [4], die attachment and high temperature binding [5]. They are specially formulated for permanent bonding to most surfaces such as metals, ceramics, glass, plastics and paper products. Even though, low thermal conductivity (T_c) of epoxy resin limit its potential use in various electronic applications. Different conductive fillers possibly from carbon sources (graphite, carbon black, carbon fibre and CNT) [6, 7], metallic (aluminium, silver, copper and nickel) [8] or ceramics (boron nitride, silicon

✉ Amit K. Singh
  singh.amit14@hotmail.com

1 Laboratory for Advanced Research in Polymeric Materials (LARPM), Central Institute of Plastics Engineering and Technology (CIPET), B-25, CNI Complex, Patia, Bhubaneswar, Odisha 751024, India

2 Central Institute of Plastics Engineering and Technology (CIPET), Chennai, India

3 Institute for Plasma Research, Gandhinagar, Gujarat, India

carbide, aluminium nitride and metal oxides) [9] have been extensively used to enhance the conductivity of epoxy based adhesives.

Nowadays carbon based fillers such as CNTs [10, 11], graphite, graphene [12, 13] and reduced graphene oxide [14] have been widely used as a conductive fillers for improving the T_c of epoxy based adhesives. Among these, CNTs have gained substantial awareness due to their high aspect ratio and large surface area which can provide percolation at a very low concentration with improving conductivity. However, high thermal resistance at the matrix-filler interface and poor dispersion in the polymer matrix limits its potential applications [15]. Numerous efforts have been made by most of researchers to get a better conductivity of CNTs–polymer matrix composites including the surface modification of CNTs [16, 17], alignment of CNTs and decoration of CNTs with conductive fillers [10, 18]. Therefore, a great consideration has been attributed to the decoration of CNTs exterior surface with metal nanoparticles [19, 20]. Among them, silver nanoparticles (Ag-NPs) [21] have gained substantial awareness due to their low cost and high T_c upto ~429 W/mK [22]. However, a very small number of information is available on the incorporation of Ag-NPs decorated onto CNT surfaces. For utilization of silver decorated CNTs in structural materials, two main issues need to be addressed: the agglomeration of silver decorated CNT occurs due to long and zigzag shape of CNTs as well as the Van-der Waals forces between them. Second, a weak interface between the Ag-NPs and CNT surfaces due to the hydrophobic nature of CNTs [23]. These consequences were effectively resolved by integrating functionalization of CNTs and ultrasonication technique which assists in de-agglomeration of CNTs.

Functionalization of CNTs with carboxylic groups is expected to increase the conductivity of polymer matrix due to its effect on the CNT dispersion in the polymer matrix and on the CNT–polymer interface. Still, there is some dispute as to the effect of CNT functionalization on the conductivity of polymer matrix. The observed trend was explained by the fact, while functionalization increases the coupling between CNTs and polymer matrix it also results in the formation of defect sites during oxidation, consequently decreased conductivity [24]. Hence, further modification was required for better interaction between functionalized CNTs and polymer matrix. The carboxylic functionalized CNTs had higher surface activity due to the presence of carboxyl groups. Hence, it is of great convenience to link other groups or atoms onto it whereas, non-functionalized CNTs surface is relatively stable and is somewhat difficult to directly modify their surfaces.

In the present work, a simple synthesis route was used to decorate MWCNTs with Ag-NPs, aiming at improving the T_c of epoxy adhesive system. For functionalization, MWCNT was treated with a mixture of concentrated sulphuric acid and nitric acid and DMF was used as a reducing agent to prepare Ag decorated MWCNT (Ag-MWCNT). Epoxy resin was used as a base matrix due to its ability to adhere to most substrates in combination with good chemical resistance, moisture resistance, electrical insulation capacity and its wide range of application in making of electronic components. The structure and morphology of Ag-MWCNTs were characterized using XRD, Raman and EDS techniques. The T_c and mechanical properties of the adhesive containing Ag-MWCNT were measured and compared to carboxyl functionalized MWCNT-epoxy adhesive system. This study intended to consider the consequence of Ag-decoration onto the properties of MWCNT filled epoxy adhesive system.

2 Materials and methods

2.1 Materials

Araldite GY 250 based on Bisphenol-A resin and Aradur HY 951 amine based curing agent was used in this work and purchased from M/s Aditya Birla Chemicals, Mumbai, India. CNTs were basically multi-walled carbon nanotubes (MWCNTs) supplied by Iljin Nanotech Co. Ltd. Korea with purity of 95%. They have an outer diameter of 20 nm and an average length of 10 μm, according to the supplier's specification. N,N-Dimethyl formamide (DMF, C_3H_7NO) and sodium dodecyl sulphate (SDS, $NaC_{12}H_{25}SO_4$) was purchased from M/s Sigma Aldrich Pvt. Ltd. India. Some common chemicals such as sulphuric acid (H_2SO_4), nitric acid (HNO_3), silver nitrate ($AgNO_3$, 0.1 mol/L) solution and acetone were purchased from M/s Merck Specialities Pvt. Ltd. Mumbai, India.

2.2 Functionalization of MWCNTs with carboxylic groups (COOH-MWCNT)

The MWCNTs (500 mg) were added to 600 ml of 3:1 (v/v) H_2SO_4 and HNO_3 acid mixture. The MWCNT–acid mixture solution was sonicated (DT-151, 3.5 L capacity M/s Darsh Technologies, India) for 6 h at 30 °C. Subsequently, the solution was diluted with deionised water (D.I.) and 0.1 M NaOH until the neutralization point was achieved. Finally, the reaction mixture was filtered through a vacuum filtration assembly fitted with a 0.2 μm PTFE filter paper followed by continuous washing with D.I. The solid precipitate obtained was vacuum dried at 80 °C for 24 h. This treatment gives rise to –COOH groups on the exterior walls of the MWCNT.

2.3 Decoration of Ag onto COOH-MWCNTs (Ag-MWCNTs)

The decoration of Ag-NPs onto COOH-MWCNT surfaces was accomplished by the reduction reaction of silver ions (Ag^+) using DMF [21]. The mechanism for the Ag^+ reduction using DMF is shown in Fig. 1.

Typically, 300 mg of COOH-MWCNTs were mixed into 250 ml of DMF and 100 mg of SDS was also added to this combination in order to improve the dispersion. The whole combination was subjected to ultrasonication for 2 h. In order to achieve the decoration of Ag-NPs onto COOH-MWCNT, 20 ml of aqueous solution of $AgNO_3$ was added drop wise to the MWCNT suspension at 60 °C with vigorous stirring. After being stirred and heated simultaneously up to 1 h, the solution was kept for another 24 h without heating or agitation. Finally, the reaction mixture was centrifuged at 2000 rpm, washed with D.I and vacuum dried at 50 °C for overnight. Figure 2 shows the schematic illustration for the formation of Ag-MWCNT.

2.4 Fabrication of epoxy conductive adhesive system

To study the effect of MWCNTs in the epoxy matrix, unmodified epoxy, COOH-MWCNT filled epoxy (epoxy-MWCNT) and Ag-MWCNT filled epoxy (epoxy-Ag-MWCNT) adhesive systems were fabricated using different wt% of fillers. To achieve better dispersion state, Ag-MWCNTs were first treated with acetone in an ultrasonication bath for 1 h. The reaction mixture was then kept in a vacuum oven at 70 °C for at least 3 h to remove the acetone completely. The treated Ag-MWCNTs were mixed with 130 g of epoxy resin using a high speed mechanical mixer at 1500 rpm for 30 min and further sonicated for 1 h to obtain homogeneous dispersion of Ag-MWCNT within epoxy resin. Finally, hardener was added to the reaction mixture maintaining 10:1 (w/w) epoxy resin: hardener ratio and homogenized. The resulting mixture was cast into a metallic mould and cured at room temperature for 24 h followed by post curing at 120 °C for 2 h.

Fig. 1 Reaction scheme for the Ag^+ reduction using DMF
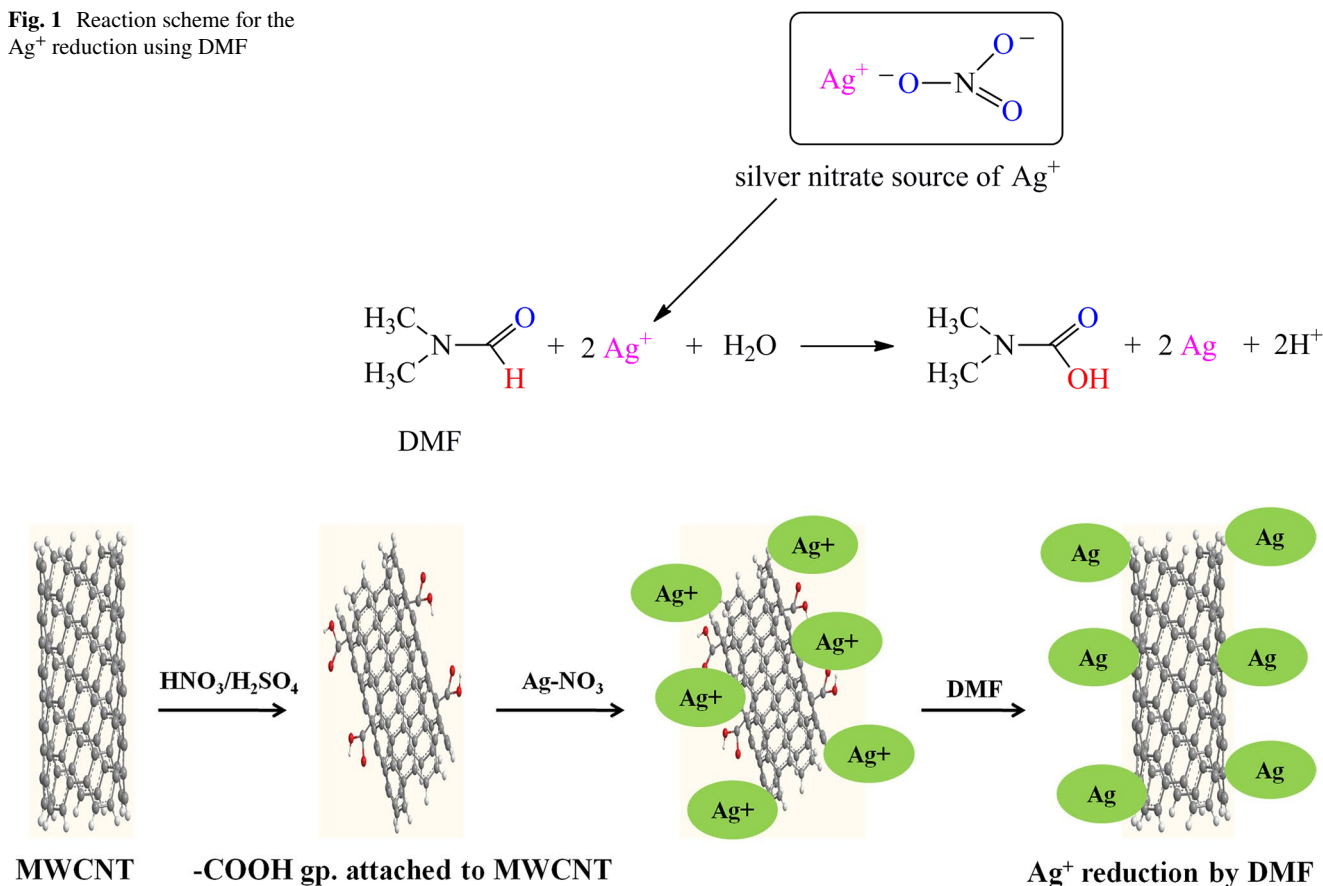
Fig. 2 Schematic illustration for the formation of Ag-MWCNTs

3 Characterization techniques

3.1 Functional group analysis

3.1.1 Fourier transform infra-red spectroscopy (FTIR)

Chemical investigation of the functional groups onto functionalized MWCNTs was carried out using Fourier transform infra-red (FTIR, Nicolet 6700, Thermo Fisher Scientific) spectroscopy. Each sample was scanned over the wavelength of 4000 to 400 cm^{-1} at a resolution of 4 cm^{-1}.

3.1.2 Raman spectroscopy

The Raman spectra of pristine and functionalized MWCNTs was carried out using a micro Raman spectrometer M/s Renishaw fitted with a Leica microscope. Excitation was provided using Argon-ion laser of 514.5 nm.

3.2 Analysis of the silver decoration onto MWCNTs

3.2.1 X-ray diffraction (XRD)

X-ray diffraction pattern of Ag-MWCNTs were recorded to confirm the presence of Ag-NPs onto the surface of COOH-MWCNTs using a powder XRD system (Shimadzu, XRD-7000L, Japan) with CuKα radiation (λ = 1.54 Å). The XRD patterns were recorded at room temperature in a continuous scan mode by recording the diffraction angle 2θ from 2° to 80°.

3.2.2 Transmission electron microscopy (TEM)

The structure and morphology of COOH-MWCNT after Ag decoration was observed using transmission electron microscope JEOL-JEM 1400, Japan. TEM images were taken at an accelerating voltage of 80 kV and sample for test was prepared by dissolving Ag-MWCNT in ethanol and drop casting onto a copper grid.

3.2.3 Energy dispersive spectroscopy (EDS)

The energy dispersive spectroscopic analysis was carried out in a JEOL-JEM 1400, Japan to analyze the chemical composition of Ag-MWCNTs. The sample was prepared by placing a drop of Ag-MWCNTs in ethanol on a copper grid and dried under ambient conditions.

3.3 Thermal conductivity measurement

The thermal conductivity of epoxy, epoxy-MWCNT and epoxy-Ag-MWCNT adhesive samples was measured according to ASTM E 1530 guarded heat flow meter method using Unitherm 2022, Anter Corpo. USA. A disc sample of diameter about 50 mm and thickness in the range of 3 mm has been prepared by using CNC cutter and tested over four different temperatures at 30, 50, 70 and 90 °C, respectively.

3.4 Scanning electron microscopy (SEM)

The morphology of fractured epoxy, epoxy-MWCNT and epoxy-Ag-MWCNT adhesive systems was analyzed using scanning electron microscope EVO MA 15 (Carl Zeiss SMT, Germany). SEM images were taken at an accelerating voltage of 20 kV and the fractured adhesive surfaces were coated with Au/Pd in vacuum.

3.5 Adhesive strength measurement

Lap shear test on the epoxy and epoxy adhesive systems were performed using Universal Testing Machine (3382 Instron, UK) at room temperature. Samples were prepared using aluminium substrate with an adhesive lap area of 12.7 mm, test grip area of 25.4 mm and tested according to ASTM D 1002 standard. The tests were performed at a cross head speed of 1.27 mm/min for at least five specimens and the mean value was reported.

3.6 Differential scanning calorimetric (DSC)

DSC studies were performed on the epoxy and epoxy adhesive systems with a TA instruments, DSC Q20 in standard DSC mode under N$_2$ atmosphere. Usually, 5–10 mg of uncured samples were dynamically cured at different heating rates of 5, 10 and 15 °C/min over a temperature range of 0–200 °C.

3.6.1 Curing kinetics behaviour

The curing kinetics study of epoxy and epoxy adhesive system allow us to determine in which temperature range, at what extent and how much heat is released during curing process. In DSC analysis, the degree of conversion (α) is proportional to the area under the exothermic peak and can be denoted as [25, 26]:

$$\alpha(t) = \frac{H_p(t)}{\Delta H} \tag{1}$$

where $H_p(t)$ is the partial heat of cure at time t and ΔH is the total heat of a cure reaction. At a given temperature (T), the rate of conversion ($\frac{d\alpha}{dt}$) is usually expressed as [27]:

$$\frac{d\alpha}{dt} = K(T)f(\alpha) \tag{2}$$

where T is the absolute temperature; $K(T)$ is the temperature dependent reaction rate constant; $f(\alpha)$ is a kinetic

model function. $K(T)$ is usually supposed to be of Arrhenius form and can be expressed as [28]:

$$K(T) = A \cdot \exp(-\frac{E_a}{RT}) \qquad (3)$$

where A is the pre-exponential factor, R is a gas constant (8.314 J/K mol), E_a is the activation energy of the reaction. In the current study, E_a is determined using Kissinger's method [25, 29]:
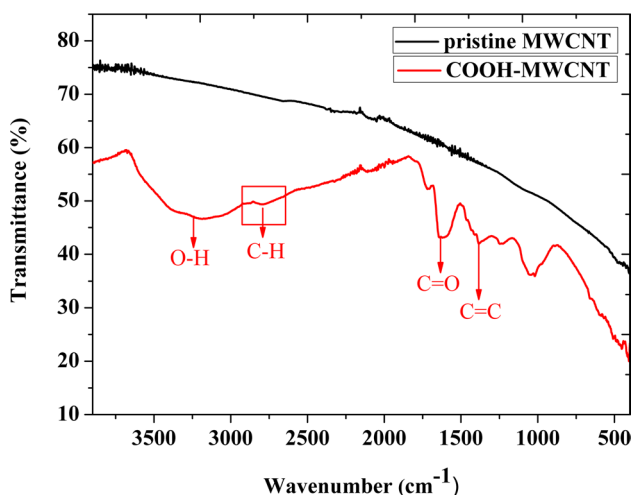
$$\ln\left(\frac{\beta}{T_P^2}\right) = C - \frac{E_a}{RT_P} \qquad (4)$$

where β is the heating rate, T_p is the maximum temperature of the exothermic peak and C is a constant. The value of E_a can be determined from the slope of an approximately linear relationship between $\ln\left(\frac{\beta}{T_P^2}\right)$ and $\frac{1}{T_p}$.

4 Results and discussion

4.1 Functionalization of MWCNTs with carboxylic groups

Figure 3 shows the relative FTIR spectrum for pristine and COOH-MWCNT. COOH-MWCNT exhibits several characteristic absorption bands of oxygen-containing groups, whereas, there were no any significant peaks noticed for pristine MWCNT. FTIR spectra collected for COOH-MWCNTs showed broad peak at ~3424 cm^{-1} which is usually attributed to the presence of adsorbed hydroxyls from H_2O, residual acids, etc. Appearance of the peak at 1723 cm^{-1} was related to the carbonyl C=O stretching vibration owing to the mild oxidation of several C-atoms due to generation of –COOH group by the reaction of sulphuric and nitric acid mixture [30–32].

The IR spectrum of COOH-MWCNTs showed prominent peaks located at 1650, 1560 cm^{-1} and in the range of 2800–2950 cm^{-1}. Peak located at 1650 cm^{-1} has been attributed to the –COOH group grafted on MWCNTs from the oxidation process [33]. Reliability of hexagonal structure of the MWCNTs was justified from the peak at 1560 cm^{-1} indicating the occurrence of double bonded carbon atoms. COOH-MWCNTs showed peak located in the range of 2800–2950 cm^{-1} which represents to the C–H symmetric and asymmetric stretching vibrations of long alkyl chains present in the surface of MWCNTs.

Figure 4 shows the typical Raman spectra of pristine and COOH-MWCNTs. The distinguished Raman characteristics for MWCNTs were Radial Breathing Modes (RBMs), D-band (ascribed to defects in disorder) and G-band (ascribed to in-plane oscillations of graphite or tangential band). The RBM is a particular characteristic to MWCNTs and it represents about the area ratio of the G-band to the D-band (I_G/I_D) indicating as oxidation affects of MWCNTs.

The spectral information of COOH-MWCNT showed two bands, D-band at 1332 cm^{-1} which was attributed to the out-of-plane sp^3-hybridized carbon vibrations and G-band can be identified at 1585 cm^{-1} which was ascribed to the in-plane C–C stretching of sp^2-hybridized carbons with I_G/I_D ratio equals to 1.18. Similarly, pristine MWCNT showed G-band at 1650 cm^{-1} and D-band at 1334 cm^{-1} with I_G/I_D ratio equals to 1.23. Lower value of I_G/I_D ratio for COOH-MWCNT reveals strong acidic treatment would be expected to increase the defect density along the side-walls of MWCNT.

Fig. 3 FTIR spectra for the pristine MWCNT and COOH-MWCNT
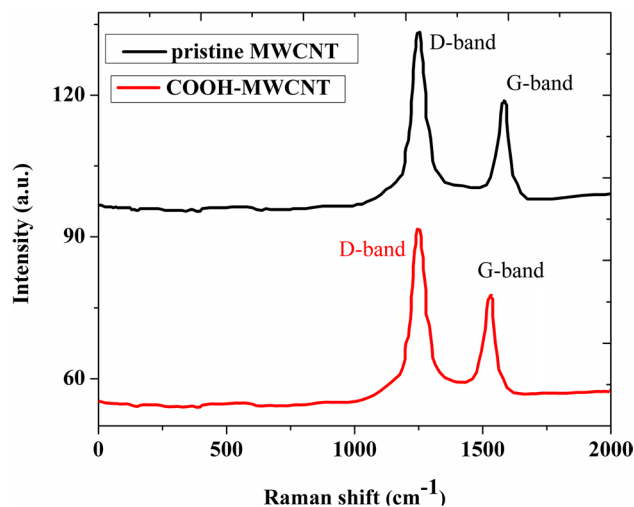
Fig. 4 Raman spectra for the pristine MWCNT and COOH-MWCNT

4.2 Decoration of COOH-MWCNT with silver nanoparticles

XRD study was performed in order to confirm the presence of Ag-NPs onto the surface of MWCNTs. the XRD pattern of pristine MWCNT and Ag-MWCNT is illustrated in Fig. 5. The XRD pattern of pristine MWCNT shows three main crystallographic planes at 26º(100), 44º(102) and 78º(110), which confirms about graphitized nature of MWCNTs. Further, Ag-MWCNT also displayed four major crystallographic planes at 38º(111), 45º(200), 64º(220) and 77º(311), analogous to the crystallographic planes of the
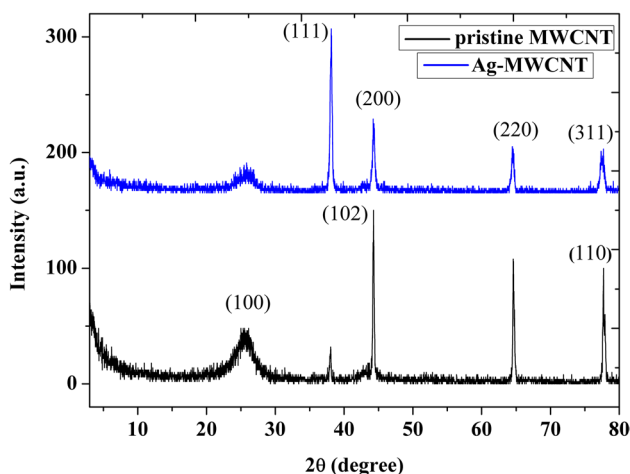

**Fig. 5** XRD spectra for the pristine MWCNT and Ag-MWCNT

face-centred cubic silver crystals [22]. Thus, the XRD pattern of Ag-MWCNT clearly demonstrated that no obvious impurities were found and the Ag-NPs formed were crystalline in nature.

Further for pristine MWCNTs, diffraction peaks were appeared at $2\theta = 38°$ and 65°, which may be assigned to iron based catalyst encapsulated into MWCNTs [34]. There were no drastic changes observed in the position of characteristics peak of pristine MWCNT and Ag-MWCNT, which suggest that MWCNTs are retained with their original structure after functionalization [35].

Figure 6 indicates TEM images for Ag-NPs decorated onto the COOH-MWCNT surfaces. It is evident from Fig. 6 that Ag-NPs embedded/decorated onto the outside wall of MWCNT having spherical in shape with average diameter around ~5–10 nm. It has been also observed that a large amount of Ag-NPs has been adhered to the MWCNTs outer surface and there was no proof of isolated Ag-NPs is noticed.

After nitration, the oxygen containing groups on MWCNTs have been employed as a nucleation centre for deposition of Ag-NPs [36]. Ag^+ in sedimentary solution of $AgNO_3$ can interact with –COOH groups on MWCNTs through non-covalent interaction by releasing H^+ ions. Some of the –COOH groups on MWCNTs sacrificed after Ag decoration; as a result Ag-MWCNTs contain less number of –COOH groups than acid treated MWCNTs [21]. The EDS spectrum in Fig. 6d shows that the sample includes the elements of Ag and C, which also demonstrated that Ag-NPs have been uniformly decorated onto

Fig. 6 TEM images for the Ag-MWCNT (**a**–**c**) and EDS spectra for the Ag-MWCNT (**d**)
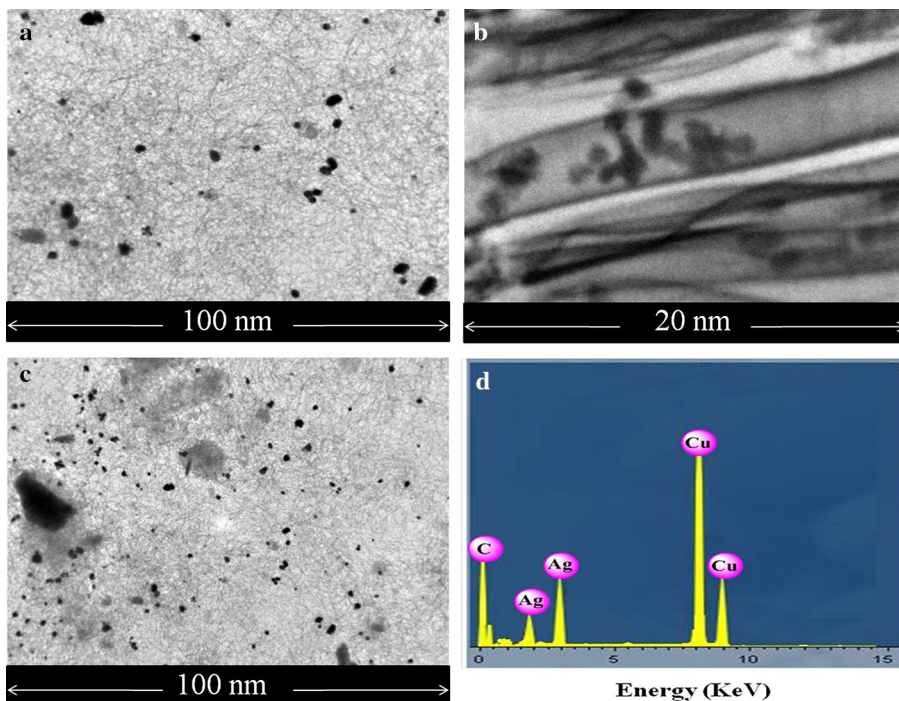
COOH-MWCNT. In the EDS spectrum, the Cu peak came from the grid specimen holder.

4.3 Thermal conductivity (T_c) measurement

The temperature dependency of the effective thermal conductivities of epoxy, epoxy–MWCNT and epoxy–Ag-MWCNT adhesive system is summarized in Table 1.

From Table 1, an increasing trend in T_c was observed with an inclusion of different surface treated MWCNTs within the epoxy matrix. T_c result as obtained demonstrates about an increasing trend for epoxy–MWCNT and epoxy–Ag-MWCNT with an increase in temperature from 30 to 90 °C. The adhesive with 0.5 wt % of MWCNT loading has resulted in the highest T_c of 0.51 W/mK at 90 °C which is 0.29 W/mK (131.8%) higher compared with unmodified epoxy whereas, at 30 °C about 78.9% increase was noticed. It is attributed that with an increase in temperature the polymer matrix begin to be expanded due to thermal expansion and conductive fillers that are networked with each other initially, becomes separated and dispersed throughout the matrix properly by making conductive paths which resulted in the improvement in the T_c values [37]. The conductivity value for epoxy–MWCNT increases slowly with an increase in the temperature. This can be attributed to the tunnelling conduction mechanism associated with MWCNTs. The presence of –COOH groups on the surface of MWCNTs may induce reduction in the tunnelling current and the conductivity will increase slightly with increasing in the temperature.

It is also expected that, decoration of MWCNTs with Ag-NPs would have a beneficial effect on the T_c of epoxy-MWCNT due to high inherent T_c of silver nanoparticles. The results obtained in Table 1 shows that the T_c is increased from 0.51 to 0.88 W/mK, after inclusion of Ag- MWCNTs. This improvement was recognized by the charge transfer involving –COOH groups and Ag^+ that were covalently-bonded onto the MWCNT surfaces (as evident from TEM images). This result signifies two major functions of Ag-MWCNTs: it behaves like a chemical agent to improve the dispersion and other, it helps in linking them thermally by producing extremely conductive layer adjoining the MWC-NTs. In such an adhesive system, a highly conductive

coating makes the major conduction path within the final system. The final efficient conductivity of the adhesive system mainly depends on the charge transfer ability of the interface between epoxy matrix and Ag-MWCNTs.

However, the T_c was noticed a decrease up to 62.9% with an addition of 1 wt% of Ag-MWCNTs as compared with 0.5 wt% of Ag-MWCNT at 90 °C. This behaviour can be justified by the two facts: the agglomeration of Ag-MWC-NTs diminishes the aspect ratio as a result, reducing the contact area between the epoxy matrix and Ag-MWCNTs and other, the Ag-MWCNT aggregation cause the occurrence of reciprocal phonon vector phenomenon, which behaves like a heat tank and limits the heat flow distribution [15, 16]. These observations implicated that the Ag-MWCNTs with unique properties can be potentially useful as the conducting filler that other filler materials rarely owns.

### 4.4 Scanning electron microscopy (SEM)

Figure 7 shows SEM images of the fractured surfaces of epoxy and epoxy conductive adhesives system. Figure 7a shows a relatively flat, smooth and featureless fractured surface indicating brittle fracture mode for pristine epoxy whereas, Fig. 7a–e depicts the fracture surface of the adhesive system made with MWCNTs and Ag-MWCNTs, respectively. Figure 7b shows the agglomeration of MWC-NTs in the epoxy matrix. In this case, microscopic cracks were observed at the interface between MWCNTs, and then continued to propagate causes the failure of whole adhesive system. MWCNT-pullout was also observed in this adhesive system, which establishes the weak interfacial bonding between the matrix and MWCNTs.

Figure 7d shows the fracture surfaces of epoxy-Ag-MWCNT adhesive system. Micrograph reveals good distribution of Ag-MWCNTs in the epoxy matrix. In this case, crack propagation initiated from the interface and Ag-MWCNTs endured from the external force were pull-out leaving behind smooth resin matrix which was exposed as strong interfacial bonding. The black arrows in these micrographs indicated the direction of crack propagation.

Also in the case of epoxy-MWCNT comparatively plain and featureless fractured surface with a nominal distance in

Table 1 Thermal conductivity value for the epoxy, epoxy-MWCNT and epoxy-Ag-MWCNT conductive adhesive systems

Temp. (ºC)	Epoxy (W/mK)	Epoxy– MWCNT (W/mK)	Epoxy–0.5%Ag-MWCNT (W/mK)	Epoxy–1%Ag-MWCNT (W/mK)
30	0.19	0.34	0.75	0.49
50	0.20	0.39	0.82	0.51
70	0.21	0.45	0.84	0.53
90	0.22	0.51	0.88	0.54
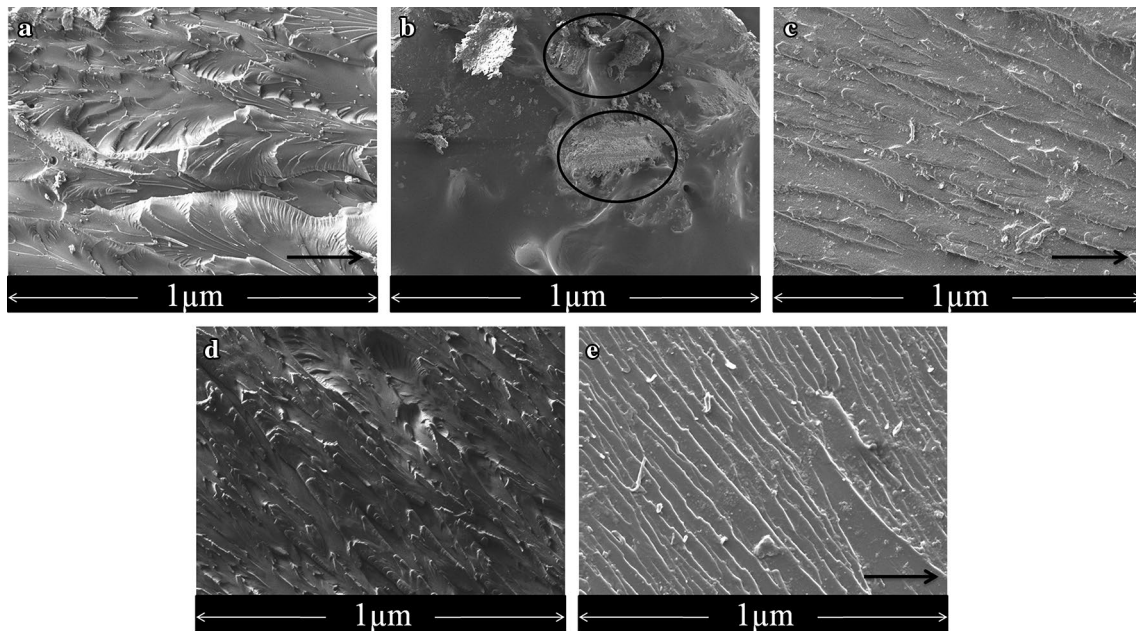
Fig. 7 SEM images of epoxy (**a**), epoxy-MWCNT (**b, c**) and epoxy-Ag-MWCNT (**d, e**) adhesive system

the range of 30–36 μm is observed between two consecutive cleavage steps (Fig. 7c) which is decreased to the range of 19–22 μm (Fig. 7e) after adding Ag-MWCNTs into unmodified epoxy. Consequentially, good shear strength by effectively forming network through bridging mechanism of MWCNTs. In our case, MWCNTs are decorated with Ag-NPs, so that Van-der Waals forces between MWCNTs become weakened. Thus, good dispersion of Ag-MWCNTs was achieved in the epoxy [17]. This also reflects probable reason for improved mechanical properties of epoxy-Ag-MWCNT compared with epoxy-MWCNT.

4.5 Differential scanning calorimeter (DSC)

The curing behaviour of the epoxy and epoxy conductive adhesives was examined using non-isothermal DSC techniques at different heating rates of 5, 10 and 15 °C/min. Figure 8a–c shows a typical DSC thermograms for epoxy, epoxy-MWCNT and epoxy-Ag-MWCNT respectively. The information showed in Table 2 shows summary result of heat of reaction (ΔH_{cure}), initial curing temperature ($T_{initial}$), peak temperature (T_{peak}) and final curing temperature (T_{final}) for epoxy, epoxy-MWCNT and epoxy-Ag-MWCNT sample.

Since curing behaviour of an epoxy resin is a function of both temperature and time, thus higher heating rates shifts the transition to a higher temperature as epoxy gets less time for changing at any explicit temperature. Thus, lower heating rate increases the resolution and higher heating rate increases the sensitivity. For all epoxy formulations, only one exothermic peak was noticed. Also, the exothermic peak height decreases in the presence of MWCNTs than that of unmodified epoxy which presents improved degree of interaction of MWCNTs with epoxy resin as well as physical hindrance caused by MWCNTs to the polymer chain mobility. The effect of MWCNT on epoxy can be established by examining ΔH_{cure}, $T_{initial}$, T_{peak} and T_{final} values. All these data have been summarized in Table 2.

It can be seen from Table 2 that ΔH_{cure} increases with increasing heating rate for all three epoxy adhesive formulations. In the case of epoxy-MWCNT adhesive a reduction in ΔH_{cure} is observed compared to pristine epoxy. As well dispersed MWCNTs can behave as a physical barrier and reduces the mobility of polymeric chain, which may results in the reduction of the total value of ΔH_{cure}. Similar results have been observed by Nusrat et al. in the case of carboxyl functionalized MWCNTs filled epoxy composite system [38]. Compared with epoxy-MWCNT, ΔH_{cure} of epoxy-Ag-MWCNT adhesive is higher. This may be due to the improved dispersion state of Ag-MWCNTs within epoxy. Also Ag decoration onto MWCNT promotes the formation of a thermal diffusion path, accelerating the dissipation of the reaction heat [29, 39]. For extra explanation on the curing behaviour of epoxy, epoxy-MWCNT and epoxy-Ag-MWCNT adhesive samples, the degree of conversion (α) as a function of temperature at 10 °C/min was plotted and shown in Fig. 9d.

In the case of unmodified epoxy, the degree of conversion (α) is higher compared to epoxy–MWCNT and epoxy–Ag-MWCNT adhesive system and gradually approaches to each other as the temperature increases.
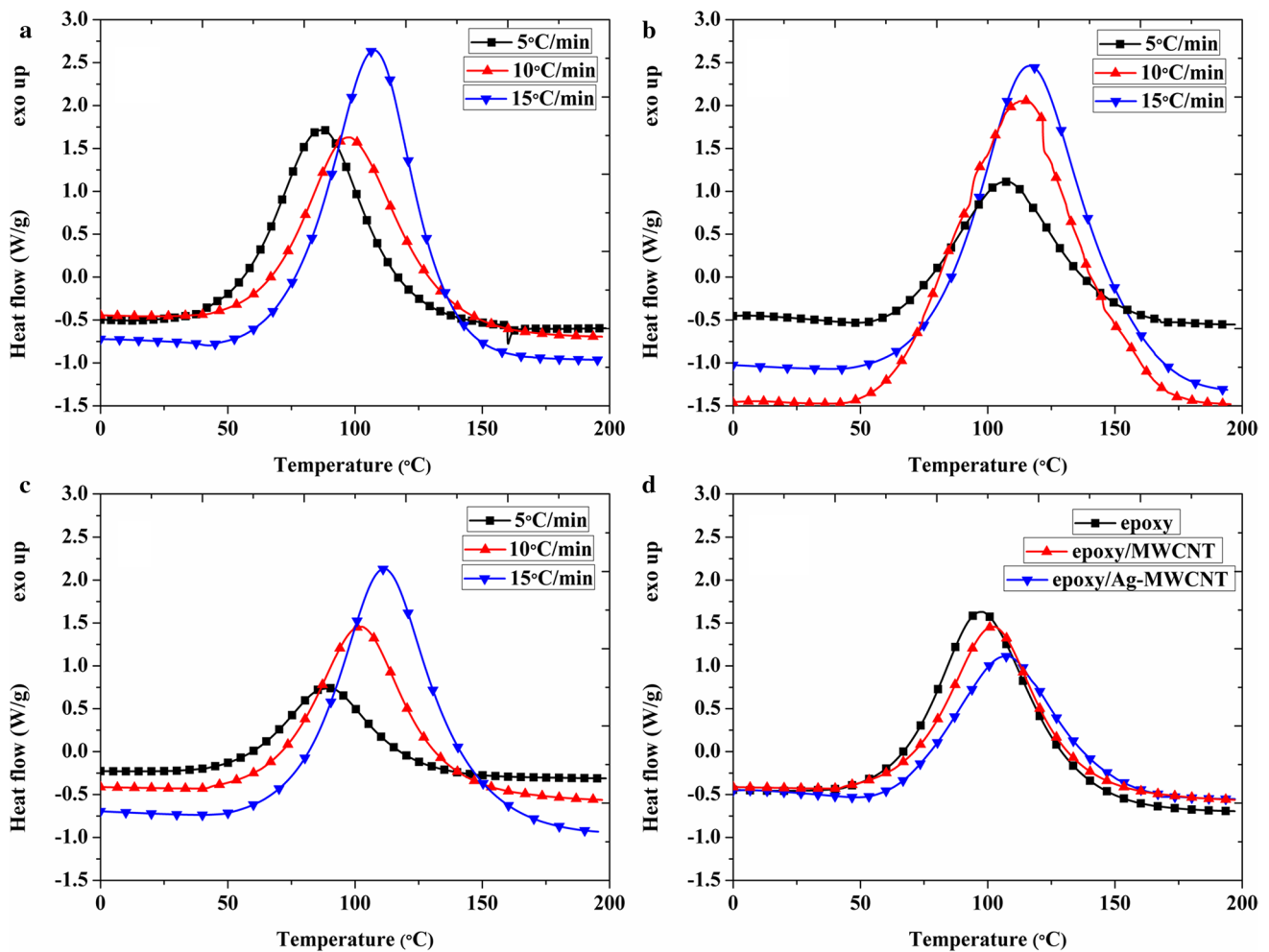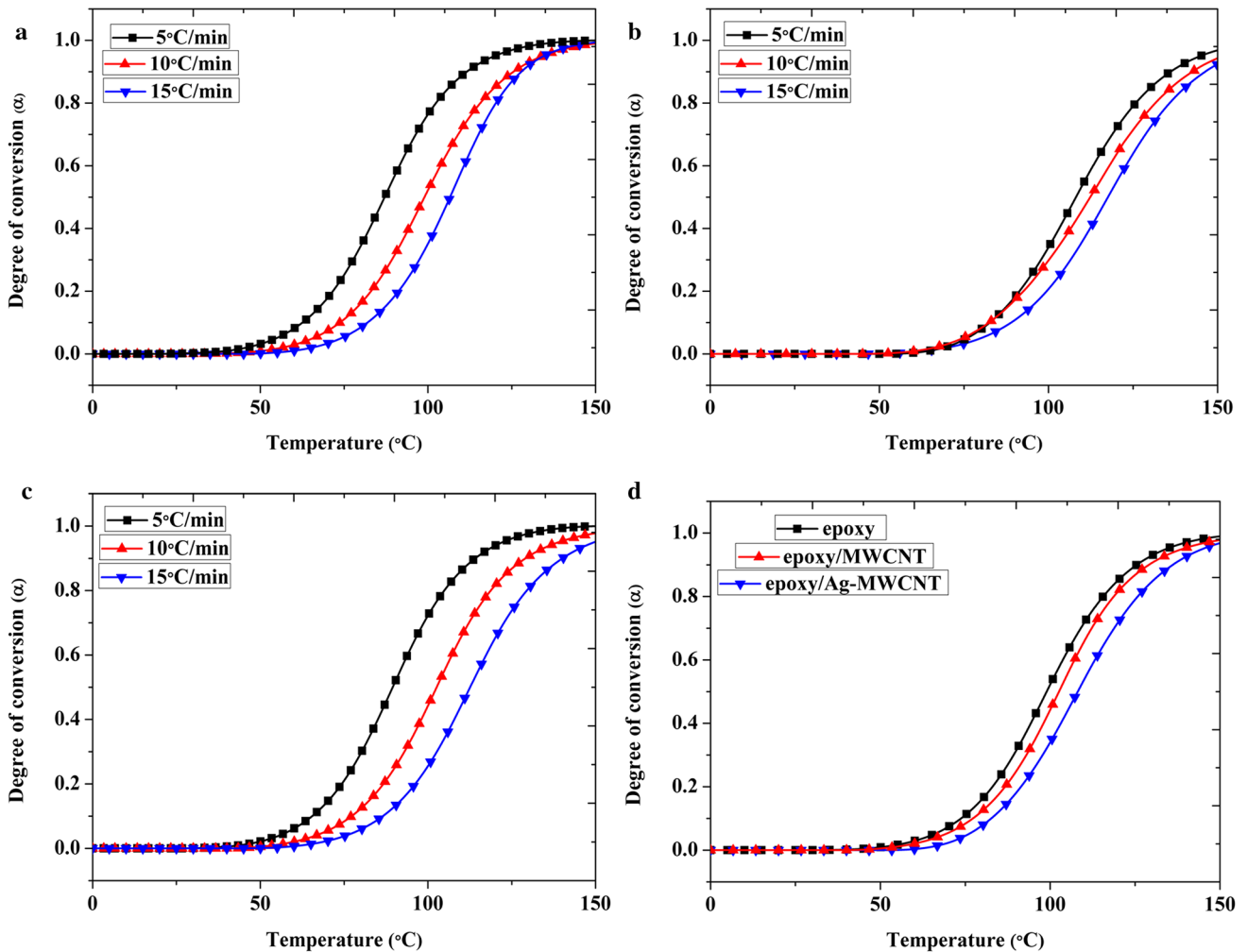
Fig. 8 Heat flow vs. temperature graph for epoxy (**a**) epoxy-MWCNT (**b**) epoxy-Ag-MWCNT (**c**) and comparison of all epoxy formulations at a heating rate of 10°C/min (**d**)

Table 2 Non-isothermal kinetic parameters obtained from DSC curves

Sample type	Heating rate β (°C/min)	$T_{initial}$ (°c)	T_{peak} (°c)	T_{final} (°c)	ΔH (J/g)
Epoxy	5	51.5	87	158.6	580
	10	62.9	98.01	178.8	586
	15	73.7	107.6	169.6	607
	5	57.2	93.9	193.8	466
Epoxy/MWCNT	10	67.3	108	193.2	489
	15	73.4	115.6	195.6	563
	5	56	90.38	166.6	524
Epoxy/ Ag-MWCNT	10	68	102.8	196.7	524
	15	76.8	111.7	195	593

The lower degree of conversion after adding MWCNT resulted in inhibition effect of MWCNTs on cross-linking process of epoxy. The mechanism behind this observation can be justified by the molecular interactions and also supported by the fact that addition of MWCNTs has

some catalytic and retardation effect due to the presence of hydroxyl groups as well as increased viscosity during initial stages of curing [40]. A sigmoid or S-shaped curve in the degree of conversion (α) versus temperature graph

Fig. 9 Degree of conversion (α) versus temperature graph for epoxy (**a**); epoxy–MWCNT (**b**); epoxy–Ag-MWCNT (**c**) and comparison of all epoxy formulations at a heating rate of 10 ℃/min (**d**)

is also observed, as expected in non-isothermal curing process.

The graph between degree of conversion (α) and conversion rate $\left(\frac{d\alpha}{dt}\right)$ is also drawn and shown in Fig. 10. Figure shows $\left(\frac{d\alpha}{dt}\right) = 0$ at initial and final stages of curing which indicated that curing reactions of epoxy adhesive systems are autocatalytic by nature. Similar results have been observed by Sahoo et al. in the case of organo modified clay filled epoxy nanocomposites [40].

### 4.5.1 Determination of activation energy (E_a)

The E_a of the epoxy, epoxy-MWCNT and epoxy-Ag-MWCNT adhesive systems was determined using Kissinger method (Eq. 4) and values obtained are summarised in the Table 3.
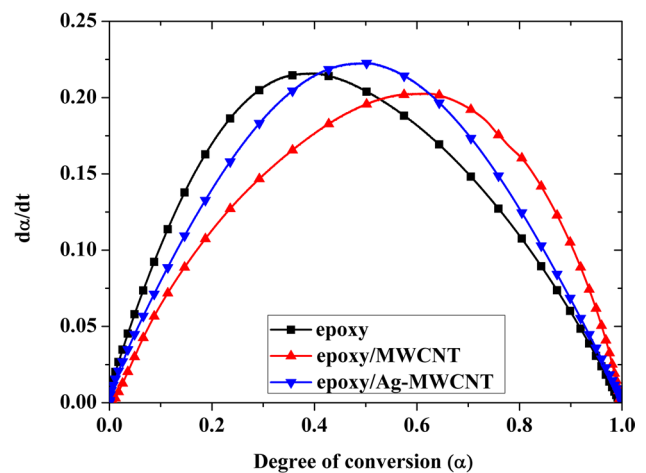
Fig. 10 Plot of degree of conversion (α) as a function of conversion rate $\left(\frac{d\alpha}{dt}\right)$ for all epoxy adhesive system at a constant heating rate of 10℃/min

**Table 3** Determination of E_a using Kissinger method at different heating rates of 5, 10 and 15 ℃/min

Sample type	Heating rate (ºC/min)			Activation energy (E_a, kJ/mol)
	5	10	15	
Epoxy	87.7	98	107.6	57.2
Epoxy–MWCNT	93.9	108	115.6	53.4
Epoxy–Ag-MWCNT	90.4	102.8	111.7	54.0
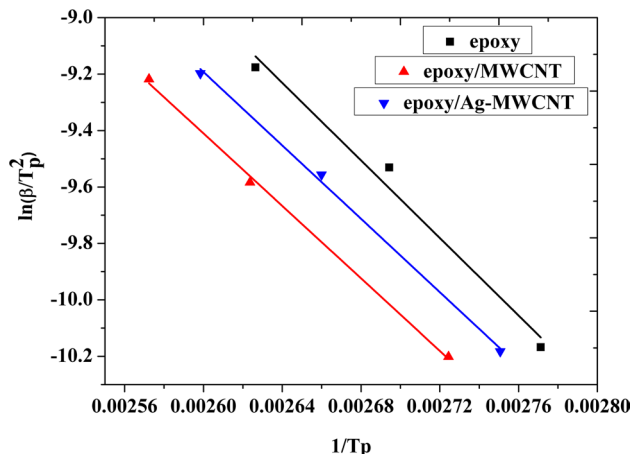
Fig. 11 Kissinger's plot for determination of E_a for epoxy, epoxy-MWCNT and epoxy-Ag-MWCNT adhesive system

Table 4 Shear strength for different epoxy adhesive system

Sample type	Shear strength (MPa)	SD
Epoxy	4.05	± 0.35
Epoxy–0.3% MWCNT	4.61	± 0.05
Epoxy–0.5% MWCNT	8.25	± 0.06
Epoxy–1% MWCNT	6.36	± 0.15
Epoxy–0.5%Ag-MWCNT	10.42	± 0.29

SD standard deviation

The value of E_a for any curing process presents the potential barrier of that reaction. E_a values calculated from Fig. 11 for epoxy, epoxy–MWCNT and epoxy–Ag-MWCNT were found to be 57.2, 53.4 and 54 kJ/mol, respectively. In case of epoxy-MWCNT, E_a was found to be much lowered compared to unmodified epoxy due to reduced viscosity which allowed better interaction of epoxy resin with amine curing agent. Enhanced distribution of amine curing agent into less viscous resin alters the curing reaction. The E_a was found to be slightly higher in the epoxy-Ag-MWCNT (only 0.6 kJ/mol) compared with epoxy-MWCNT adhesives, which might be due to the fact that decoration of Ag-NPs onto MWCNTs hinders the curing process of the epoxy system.
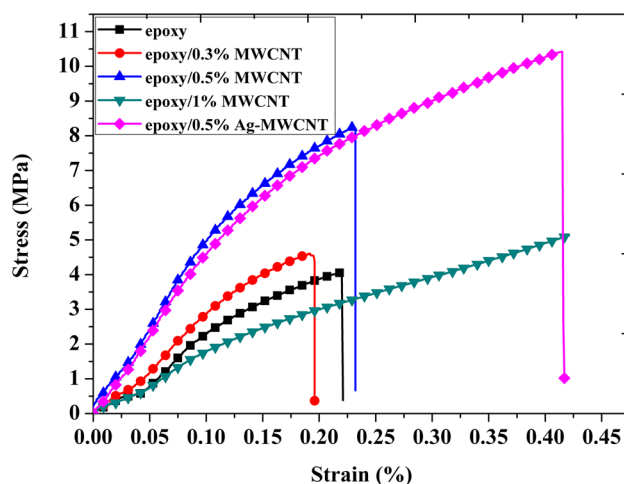
**Fig. 12** Stress versus Strain curve for epoxy and epoxy nano-conductive adhesive system

4.6 Adhesive strength measurement

Lap shear tests were performed to evaluate the effect of MWCNTs on the properties of epoxy adhesive system. The results of lap shear tests are presented in Table 4 and the stress–strain curves for different epoxy adhesive systems are shown in Fig. 12.

From Table 4, it is clear that increasing the wt% of MWCNTs (from 0 to 0.5 wt %) resulted in increase in the strength of the epoxy adhesive systems. With an addition of 0.5 wt % of MWCNTs into unmodified epoxy resulted as significant improvement in the shear strength up to 8.25 MPa, which is 4.05 MPa (approx. 104%) higher compared to pristine epoxy. Enhancement in the mechanical properties of the epoxy-0.5% MWCNT adhesive system was due to the homogeneous dispersion and good interaction between MWCNTs and the epoxy matrix [41, 42]. While, by adding 1 wt% of MWCNTs, the epoxy adhesive strength decreases upto 29.7% compared with epoxy-0.5% MWCNT. This decrease may be attributed to the aggregation of MWCNTs and stress concentration in the agglomeration areas which initiates the crack propagation in the epoxy adhesive system. However, the strength of the epoxy adhesive comprising Ag-MWCNTs were constantly higher than pristine MWCNTs, signifying the strengthening effect due to MWCNTs in epoxy adhesives was not sacrificed after Ag decoration. Silver decoration onto the MWCNTs has shown a drastic increase in the strength of about 6.37 MPa compared to 0.5 wt% loading of MWCNTs adhesive system.

Ag-MWCNTs have the possibility to be more effective as reinforcing agent than pristine MWCNTs as surface modified MWCNTs consist of reactive sites as a result homogeneous dispersion within polymer matrix [11, 43].

Fig. 13 Mode of failure of epoxy (**a**) epoxy–MWCNT (**b**) and epoxy-Ag-MWCNT (**c**) conductive adhesive system

Adhesive on one side   Adhesive on both sides   Adhesive on one side
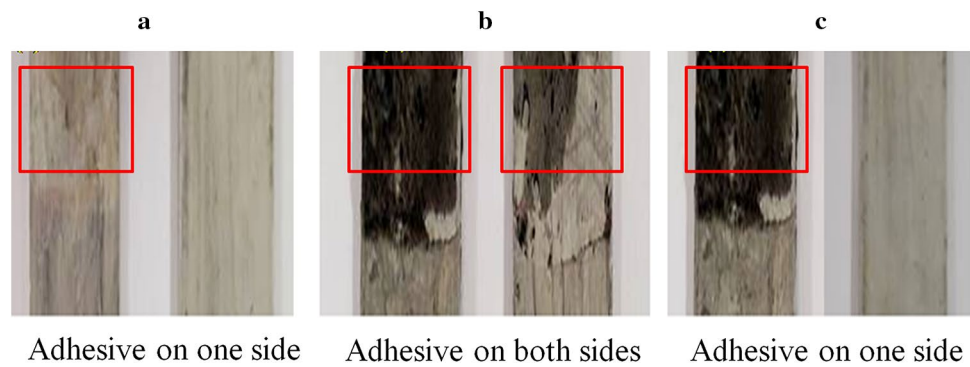
During the curing process the Ag$^+$ attached to the surface of Ag-MWCNTs reacts with the epoxy and forms a covalent linkage which causes to higher strength of the epoxy adhesives. Ag-MWCNTs have better dispersion in the epoxy, which indicates that, a good interfacial bonding enables an effective stress transfer between the epoxy matrixes. Thus 0.5 wt% Ag-MWCNT containing epoxy adhesive system has a higher strength than that of epoxy-0.5% MWCNT. Similar findings were observed by Ma et al. [22].

Linear stress–strain relation was noticed in all the epoxy adhesive samples before the stress level reaching to the maximum value. All the samples imparted brittle failure indicated by a sudden drop in the peak stress.

4.7 Type of fracture of epoxy adhesive after lap shear test

The mode of failure of the epoxy and epoxy conductive adhesives are shown in Fig. 13. It is detected that the mode of failure for unmodified epoxy is adhesive (Fig. 13a). An adhesive failure occurs at the interface between the adhesive and the adherent with the entire adhesive on one side of the substrate material. This depicts brittle failure mode of epoxy adhesives on substrates. Hence, a relationship between the adhesive failure and the stress–strain response of an adhesive is established. These considerations are in good agreement with low shear strength of pristine epoxy.

Whereas, for the epoxy–MWCNT adhesive the mode of failure was cohesive as well (Fig. 13b). It occurs at the interface between the adhesive and the substrate. The mode of failure progressed from adhesive to cohesive for epoxy-Ag-MWCNT (Fig. 13c). This mode of failure indicates the relaxation of stress during buckling occurs not only in the delaminated sections, but also within the stress transfer zones [44]. This relation is confirmed by the higher strain percentage at break of epoxy-Ag-MWCNTs adhesive system.

5 Conclusions

In this work a simple approach for the Ag decoration onto carboxyl functionalized MWCNTs using DMF as a reducing agent have been reported. The presence of oxygen containing functional groups in FTIR and principal bands in Raman spectroscopy concluded that carboxyl groups have been uniformly anchored onto the MWCNT surfaces. Furthermore, XRD, TEM and EDS studies additionally corroborated the structure and morphology of Ag-MWCNTs. The thermal conductivity of epoxy adhesives can be effectively increased with 0.5 wt% loading of Ag-MWCNT. This increase may be attributed to good compatibility; well distribution and high surface area of MWCNTs resulted in the formation of heat flow network and thereby have extended area of epoxy-Ag-MWCNTs contact. Additionally, a 5.37 MPa enhancement in lap shear strength was observed for epoxy-Ag-MWCNT with 0.5 wt% loading of Ag-MWCNT as compared with unmodified epoxy, which has been justified on account of SEM micrographs.

The curing kinetics of epoxy adhesive systems were also investigated employing non-isothermal DSC analysis. Test results showed that the E_a decreased with the addition of conductive fillers within epoxy which might be due to the hindrance of molecular movement of epoxy resin. Based on these results, it can be concluded that the Ag-MWCNTs is a promising candidate for the improvement of various properties of unmodified epoxy.

References

1. L. Chen, P. Zhao, H. Xie, W. Yu, Compos. Sci. Technol **125**, 17 (2016)
2. F.L. Guan, CX. Gui, HBin Zhang, ZG. Jiang, Y. Jiang, Z.Z. Yu, Composites B **98**, 134 (2016)

3. A. Larmagnac, S. Eggenberger, H. Janossy, J. Voros, Sci. Rep. **4**, 7254 (2014)
4. T.M. Cornsweet, Science **168**, 433 (1970)
5. M.J. Hanus, A.T. Harris, Prog. Mater. Sci. **58**, 1056 (2013)
6. V. Causin, C. Marega, A. Marigo, G. Ferrara, A. Ferraro, Eur. Polym. J. **42**, 3153 (2006)
7. S. Yu, P. Hing, X. Hu, Science **33**, 289 (2002)
8. C.V. Bouanga, T.F. Heid, M.F. Frechette, E. David, Elecrical Insul. Dielectr. Phenom. ,709 (2015) doi:10.1109/CEIDP.2015.7352138
9. H. Ishida S. Rimdusit, Thermochim. Acta **320**, 177 (1998)
10. E.S. Choi, J.S. Brooks, D.L. Eaton, M.S. Al-Haik, M.Y. Hussaini, H. Garmestani, D. Li, K. Dahmen, J. Appl. Phys **94**, 6034 (2003)
11. E. Fortunati, F.D. Angelo, S. Martino, A. Orlacchio, J.M. Kenny, I. Armentano, Carbon. (2011). doi:10.1016/j.carbon.2011.02.004
12. Y.X. Fu, Z.X. He, D.C. Mo, S.S. Lu, Int. J. Therm. Sci **86**, 276 (2014)
13. N.K. Mahanta, M.R. Loos, I. Manas Zlocozower, A.R. Abramson, J. Mater. Res. **30**, 959 (2015)
14. T. Huang, X. Zeng, Y. Yao, R. Sun, F. Meng, J. Xu, C. Wong, RSC Adv. (2016) doi:10.1039/C5RA27315C
15. P. Kim, L. Shi, A. Majumdar, P.L. McEuen, Phys. Rev. Lett. **87**, 215502 (2001)
16. S.Y. Yang, C.C.M. Ma, C.C. Teng, Y.W. Huang, S.H. Liao, Y.L. Huang, H.W. Tien, T.M. Lee, K.C. Chiou, Carbon **43**, 592 (2010). doi:10.1016/j.carbon.2009.08.047
17. F. Xin, L. Li, Composites A **42**, 961 (2011)
18. H. Huang, C. Liu, Y. Wu, S. Fan. Adv. Mater. **17**, 1652 (2005)
19. N. Alexeyeva, J. Kozlova, V. Sammelselg, P. Ritslaid, H. Mandar, K. Tammeveski, Appl. Surf. Sci. **256**, 3040 (2010)
20. Q. Liu, W. Ren, Z.G. Chen, B. Liu, B. Yu, F. Li, H. Cong, H.M. Cheng, Carbon **2**, 1722 (2008). doi:10.1016/j.carbon.2008.06.021
21. F. Ahmadpoor, S.M. Zebarjad, K. Janghorban, Mater. Chem. Phys. **139**, 113 (2013)
22. P.C. Ma, B.Z. Tang, J.K. Kim, Carbon **46**,1497 (2008). doi:10.1016/j.carbon.2008.06.048
23. B. Munkhbayar, M.R. Tanshen, J. Jeoun, H. Chung, H. Jeong, Ceram. Int. **39**, 6415 (2013)
24. R. Gulotty, M. Castellino, P. Jagdale, A. Tagliaferro, A.A. Balandin, ACS Nano **7**, 5114 (2013)
25. M.A. Vargas, H. Vazquez, G. Guthausen, Thermochim. Acta **611**, 10 (2015)
26. J. Hu, J. Shan, J. Zhao, Z. Tong, Thermochim. Acta **632**, 56 (2016)
27. S. Montserrat, J. Malek, Thermochim. Acta **228**, 47 (1993)
28. W. Fang, X. Jun, W. Jing-wen, L. Shu-qin, High Perform. Polym. **24**, 730 (2012)
29. T. Zhou, X. Wang, X. Liu, D. Xiong, Carbon **48**, 1171 (2009). doi:10.1016/j.carbon.2008.12.039
30. S.-Y. Lee, S.J. Park, Bull. Korean Chem. Soc. **31**, 1596 (2010)
31. S. Chen, W. Shen, G. Wu, D. Chen, M. Jiang, Chem. Phys. Lett. **402**, 312 (2005)
32. R. Yudianti, H. Onggo, Y. Saito, T. Iwata, J. Azuma, Open Mater. Sci. J. **5**, 242 (2011)
33. M.A. Atieh, O.Y. Bakather, B. Al-Tawbini, A. A. Bukhari, F.A. Abuilaiwi, M.B. Fettouhi, Bioinorg. Chem. Appl. **2010**, (2010)
34. G. Grassi, A. Scala, D. Iannazzo, A. Piperno, Chem. Commun. **48**, 6836 (2012)
35. S.H. Pisal, N.S. Harale, T.S. Bhat, H. Dshmukh, P.S. Patil, IOSR J. Appl. Chem. **7**, 49 (2014)
36. T.W. Ebbeser, H. Hiura, M.E. Bisher, M.M.J. Treacy, J.L. Shreeve-keyer, R.C. Haushalter, adv. mater. **8**, 155 (1996) doi:10.1002/adma.19960080212
37. Q. Li, Q.Z. Xue, X.L. Gao, Q.B. Zheng, Express. Polym. Lett. **3**, 769 (2009)
38. N. Jahan, A.T. Narteh, M. Hosur, M. Rahman, S. Jeelani, Open J. Compos. Mater. **3**, 40 (2013)
39. L.J. Cui, Y. Bin Wang, W.J. Xiu, W.Y. Wang, L.H. Xu, X.B. Xu, Y. Meng, L.Y. Li, J. Gao, L.T. Chen, H.Z. Geng, Mater. Des. **49**, 279 (2013)
40. S.K. Sahoo, S. Mohanty, S.K. Nayak, Thermochim. Acta. **614**, 163 (2015)
41. M.T. Le S.C. Huang, Materials. **8**, 5526 (2015)
42. F.H. Gojny, K. Schulte, Compos. Sci. Technol. **64**, 2303 (2004)
43. G.V. Ramana, B. Padya, R.N. Kumar, K.V. Prabhakar, P.K. Jain, Indian J. Eng. Mat. Sci. **17**, 331 (2010)
44. P. Jojibabu, M. Jagannatham, P. Haridoss, G.D. Janaki Ram, A.P. Deshpande, S.R. Bakshi, Composites A **82**, 53 (2016)